Surfactant Assembly within Pickering Emulsion Droplets for Fabrication of Interior-Structured Mesoporous Carbon Microspheres

Dawei Liu, Nan Xue, Lijuan Wei, Ye Zhang, Mingxing Tang, Xuekuan Li, Bernard P. Binks, and Hengquan Yang*

Abstract: Large-sized carbon spheres with controllable interior architecture are highly desired, but there is no method to synthesize these materials. Here, we develop a novel method to synthesize interior-structured mesoporous carbon microspheres (MCMs), based on the surfactant assembly within water droplet-confined spaces. Our approach is shown to access a library of unprecedented MCMs such as hollow MCMs, multi-chambered MCMs, bijel-structured MCMs, multi-cored MCMs, "solid" MCMs, and honeycombed MCMs. These novel structures, unattainable for the conventional bulk synthesis even at the same conditions, suggest an intriguing effect arising from the droplet-confined spaces. This synthesis method and the hitherto unfound impact of the droplet-confined spaces on the microstructural evolution open up new horizons in exploring novel materials for innovative applications.

Carbon spheres are one of the most important materials for catalysis, separation, and energy storage.[1] Driven by their appealing applications, various carbon spheres with hollow,[2] yolk–shell,[3] and multi-shell[4] architectures have been successfully fabricated. However, these achievements are largely limited to nanometer-sized carbon microspheres. In fact, for many practical applications, micron-sized spheres are highly desirable because of easy processing and separation compared to nanospheres.[5] More desirable is those mesoporous carbon microspheres that possess a hierarchical or multi-compartmentalized interior structure because such a structure can significantly benefit mass transport-relevant processes[6] and enable spatio-temporal control of a chemical process occurring in their interior.[7]

However, fabrication of interior-structured mesoporous carbon microspheres (MCMs) is extremely challenging in comparison to carbon nanospheres because it is non-trivial to realize delicate control of their interior structure. Although spraying,[8] emulsion,[9] aerosol-assisted self-assembly[5a] and dripping[10] methods have been explored to prepare carbon materials, these approaches are usually limited to producing spherical particles of sizes ranging from sub-micron to a few microns.[8,9a] Moreover, the resultant carbon microspheres fail to possess complex interior structures because of the inability of these methods in diversifying the assembly at a micron scale.

Herein, we report a novel approach to attain this goal. This approach mainly involves independent formation of crust and interior architectures. Water droplets in nanoparticle-stabilized emulsions (Pickering emulsions) are used as spherical templates to grow outer crusts because they are of much higher stability than conventional surfactant-stabilized droplets.[11] The surfactant-directed assembly inside the Pickering water droplets is capitalized to create internal structures. Since nanoparticle emulsifier and surfactants differ significantly in nature, our strategy makes it possible to optionally tailor the interior structure of MCMs through changing synthesis conditions, while not affecting the outer crust. To the best of our knowledge, for the first time, surfactant assembly inside Pickering droplets is proposed to synthesize materials although Pickering droplets were previously reported to be used as spherical templates to fabricate polymer microspheres.[12] Our method is shown to access a library of unprecedented micron-sized carbon spheres with novel interior structures including hollow MCMs, multi-chambered MCMs, bijel-structured MCMs, multi-cored MCMs, "solid" MCMs, and honeycombed MCMs.

The synthesis process started with preparation of a water-in-oil Pickering emulsion by homogenizing a mixture of toluene and water in the presence of phenolic resol (oligomer), NaOH, silica particles (Pickering emulsifier) and the amphiphilic triblock polymer Pluronic F127. Subsequently, polymerization at oil-water interfaces and within water droplets took place at 80–110 °C, forming polymer microspheres. After carbonization at 600 °C MCMs were obtained. The morphology and internal structure of the obtained samples were characterized by scanning electron microscopy (SEM). For example, the sample synthesized at 0.4 mol L^{-1} NaOH (100 °C, 30 wt% phenol) consists of discrete, regular spheres of 60–80 μm in size and their surfaces are relatively smooth (Figures 1A,B). From their cross-sections, one can see there are numerous uniform small spheres of ca. 5 μm inside the hollow microsphere (Figures 1C,D). The crust thickness of hollow microspheres is 2–3 μm (Figure S1). This material is accordingly denoted as multi-cored MCMs. Transmission electron microscopy (TEM) images (Figures 1E,F) show large domain regularity with a well-ordered body-centered

[a] Dr. D. Liu, Y. Zhang, M. Tang, Prof. X. Li
State Key Laboratory of Coal Conversion, Institute of Coal Chemistry, Chinese Academy of Sciences
Taiyuan 030001, China
[b] Dr. D. Liu, N. Xue, L. Wei, Prof. H. Yang
School of Chemistry and Chemical Engineering, Shanxi University
Taiyuan 030006, China
E-mail: hqyang@sxu.edu.cn
[c] Dr. D. Liu, M. Tang
University of Chinese Academy of Sciences
Beijing 100049, China
[d] Prof. B. P. Binks
School of Mathematics and Physical Sciences, University of Hull
Hull HU6 7RX, United Kingdom

Supporting information and the ORCID identification number(s) for the author(s) of this article can be found under http://dx.doi.org/10.1002/anie.xxxxxxxxx

cubic ($Im\bar{3}m$) mesostructure. Their N_2 sorption isotherm shows a typical type-IV curve and two hysteresis loops (Figure 1G). The

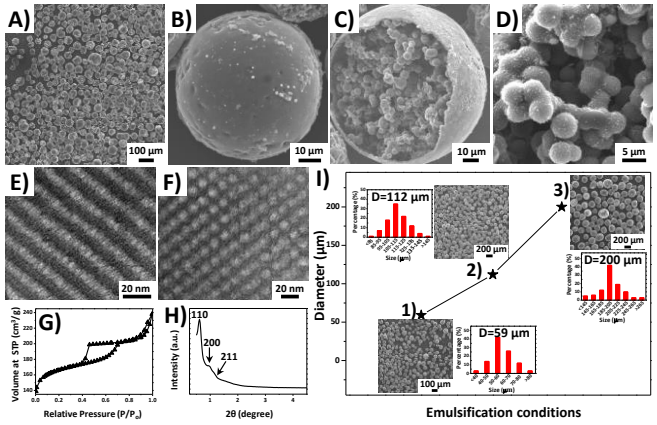

Figure 1. A–H) Characterization of multi-cored MCMs. A) Low magnification SEM image. B) SEM image for a single microsphere. C) SEM image showing the interior structure of microsphere cut deliberately. D) High magnification SEM image showing its interior structure. E) TEM image viewed from [110] direction. F) TEM image viewed from [100] direction. G) N_2 adsorption-desorption isotherm. H) Small-angle XRD pattern. I) SEM images and tuning of MCMs size through varying emulsification conditions: (1) 25,000 rpm, 2.5 wt% silica emulsifier; (2) 8,000 rpm, 2.5 wt% silica emulsifier; (3) 8,000 rpm, 1.5 wt% silica emulsifier.

former hysteresis loop belongs to an H1-type and the latter features an H3-type. They correspond to mesopores and the void spaces arising from stacking of inner carbon nanospheres, respectively. The specific surface area, pore volume and pore size of MCMs were determined respectively to be 580 $m^2 g^{-1}$, 0.36 $cm^3 g^{-1}$ and 7 nm (Figure S2). The pore size is much larger than those of typical mesoporous carbon materials,[13] due to the swelling effects caused by toluene. The small-angle X-ray diffraction (XRD) pattern exhibits an intense diffraction peak at $2\theta = 0.6^o$ together with two weak diffraction peaks at 0.9^o and 1.2^o (Figure 1H). These peaks can be indexed as (110), (200) and (211) reflections of body-centered cubic $Im\bar{3}m$ symmetry,[14] which is in agreement with the TEM results. Notably, after removal of the initially added silica emulsifier from the surfaces of MCMs using HF, their morphology, interior structure and ordered mesopores were well preserved, and the surface area and pore volume gained a slight increase (Figure S3).

Interestingly, we found that the interior structure of MCMs strongly depended on the base concentration applied although the spherical morphology was not altered. When decreasing the NaOH concentration from 0.4 to 0.2 mol L^{-1}, plenty of macropores of 1.5–3.0 μm appear. The macropores are distributed homogeneously throughout the interior of the microspheres (Figures 2A and S4A; referred as to multi-chambered MCMs). Increasing the NaOH concentration up to 0.6 and then to 0.8 mol L^{-1} led to "solid" microspheres (Figures 2A, S4C and S5). Their ordered mesoporous structures are also confirmed by N_2 sorption analysis (Figure S4D), XRD measurement (Figure S4E) and TEM observation (Figure S4F).

In parallel, we found that when the polymerization temperature was decreased from 100 down to 80 and 90 °C or increased up to 110 °C (0.4 mol L^{-1} NaOH, 30 wt% phenol), the interior structure and external surface underwent a considerable change. For the MCMs synthesized at 80 °C, there are many homogeneously distributed micrometer-sized holes on their external surface (Figure S6A). Interestingly, their interior exhibits a coarsened bijel (bicontinuous) structure,[15] in which many gullies are three-dimensionally interconnected (Figures 2B and S6A). When the polymerization temperature was increased to 90 °C, the holes on the external surface nearly disappeared and the bijel interior structure was more pronounced (Figures 2B and S6B). When the polymerization temperature was raised to 110 °C, a honeycombed structure was observed within microspheres (Figures 2B and S6C). N_2 sorption analysis confirmed their mesoporous structures (Figure S7).

Another interesting observation is that the dosage of carbon precursor also induced changes in the interior structure. When a limited amount of phenol (7.5 wt%, 0.4 mol L^{-1} NaOH, 100 °C, molar ratio of phenol to formaldehyde was fixed at 1:2 for all cases) was used, crumpled hollow MCMs with crust thickness of about 1 μm were obtained (Figures 2B and S8B). It is worth mentioning that this crust still possesses a mesoporous structure, which is confirmed by XRD (Figure S9A), N_2 sorption analysis

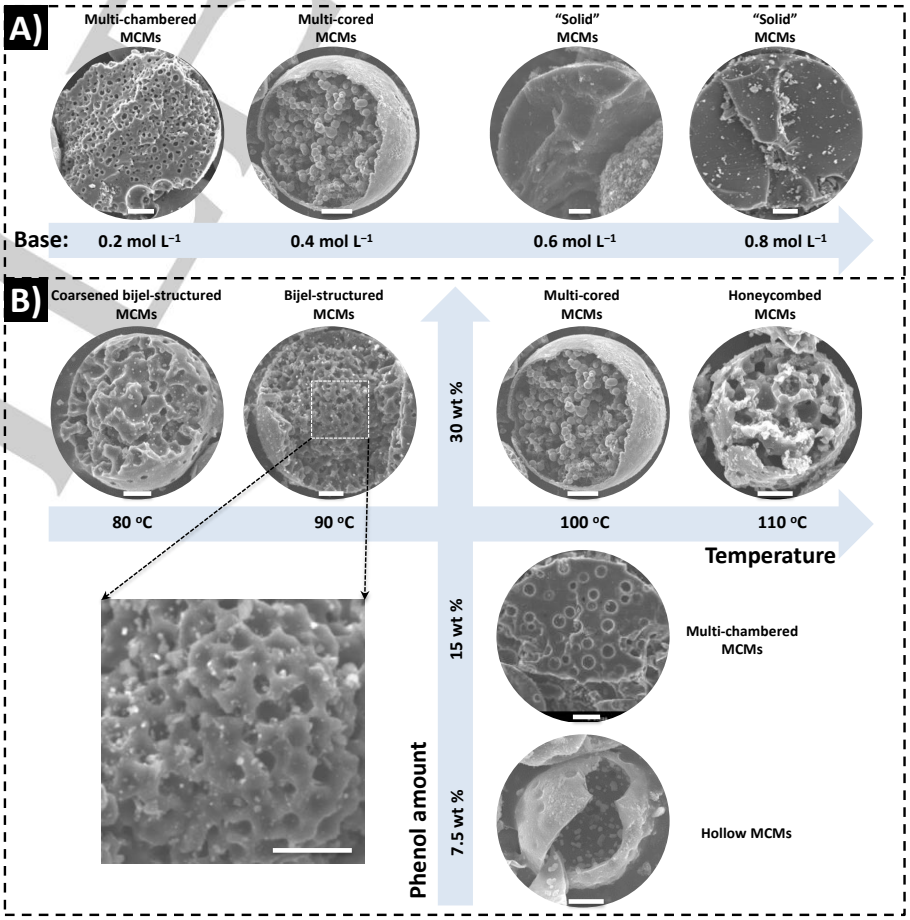

Figure 2. SEM images showing the interior structural evolution of MCMs as a function of A) base concentration, and B) temperature and amount of phenol. Scale bar = 40 μm.

(Figure S9B) and TEM observation (Figure S10). Increasing the phenol amount to 15 wt% led to multi-chambered MCMs (Figures 2B and S8A). When the phenol amount reached 30 wt%, multi-cored MCMs were produced (earlier).

Besides the interior structure, the size of MCMs can be tuned through variation of the size of the water droplets. It is well known that higher particle concentration and higher stirring speed lead to smaller Pickering emulsion droplets.[16] Following this principle, the average diameter of resultant MCMs can be tuned from 59 μm to 200 μm (Figure 1I), highlighting the additional flexibility of our synthesis protocol. It is worth emphasizing that each type of MCM has good structural homogeneity, which is confirmed by multiple SEM images for each sample (Figures S11 and S12). It is not surprising when one considers that each individual droplet provides a very similar microenvironment for the structural evolution, ensuring the high uniformity.

Given such a diversity of the interior structures, we are aware of the uniqueness of the underlying mechanism for the structural evolution. The phenolic resol oligomers co-assemble with F127 through hydrogen bonding interactions, forming nanomicelle composites within the water droplets.[14] These composites migrate towards the oil/water interface, deposit there and further grow into mesoporous structures around the inner surfaces of water droplets (Figure 3A). This is because the liquid-liquid interface can induce heterogeneous nucleation, which requires a lower energy in comparison to homogeneous nucleation.[17a] The preferential growth of the shell is supported by a control experiment, in which a limited amount of phenol (7.5 wt%) leads to a crust alone (Figure 2B). As such, the surface of each droplet acts as geometric template for growing a spherical crust. This is confirmed by another control experiment, in which the absence of droplets led to irregular morphology (Figures S13 and S14). Besides directing the ordered mesoporous structure, the presence of F127 helps to form smooth surfaces, which is supported by the F127-free experiment (Figure S15). When the concentration of nanomicelle composites within water droplets reaches a certain threshold value, homogeneous nucleation and growth within the droplet-confined spaces begins to occur (Figure 3B). It is should be noted that amphiphilic F127 can stabilize small oil drops within the water droplets, forming an oil-in-water-in-oil (O/W/O) multiple emulsion. This is validated by optical microscopy observation (Figure S16A). Due to the high Laplace pressure,[17b] these oil drops are stable only at relatively low temperatures or low base concentrations. The presence of toluene drops inside water droplets leads to a multi-chambered structure because the polymerization of nanomicelle composites takes place outside the inner toluene drops. Under certain conditions, induced by the polymerization, the enclosed liquid mixture including toluene, water, nanomicelle composites and F127 undergoes microphase change via spinodal decomposition,[18a] yielding a bijel (bicontinuous) phase. The polymerization facilitates the instant solidification and arrest of a local metastable phase of the viscous liquids, yielding bijel-structured MCMs. Because the solidification rate is relatively slow at 80 °C, a coarsened bijel structure is captured. At 90 °C its rate increases, leading to a finer bijel structure. As polymerization proceeds, the inner toluene is hunted out, generating holes on the surface of MCMs, as evidenced by the SEM images in Figure S6A. Upon increasing the temperature or increasing the concentration of base, inner toluene drops cannot form at the beginning (Figure S16B) and the confined space becomes a completely aqueous environment. High base concentration and high temperature promote formation of more nuclei, which subsequently grow into nanospheres within the hollow MCMs (multi-cored MCMs). When increasing the NaOH concentration up to 0.6 mol L^{-1}, oligomers bear more charges.[18b] As a result, all the oligomers are distributed within water droplets. More precursors available for polymerization lead to a monolith structure within the confined spaces ("solid" MCMs), which is supported by the mass measurement of the resultant polymer microspheres (Table S1). When the temperature reaches 110 °C, gaseous water is generated and small bubbles form inside the water droplets. These small bubbles can be stabilized by amphiphilic F127 molecules or nanomicelle composites by adsorption at their surface. This case leads to a honeycombed interior structure (honeycombed MCMs). These microstructures form during polymerization, which is confirmed by their SEM images captured for the polymers (Figures S17 and S18).

Such a unique mechanism is related to the droplet-confined spaces. This is supported by comparison with synthesis in bulk systems (Figures S13 and S14). Using bulk systems (the synthesis conditions are exactly the same conditions as those in emulsion systems), the honeycombed, coarsened bijel, pronounced bijel, and multi-cored structures were not obtained, but instead irregular particles without complex microstructures were generated. Such an impact is understandable when considering microphase changes. In the confined spaces created by the droplets and subsequent solid crusts where the efflux and influx are

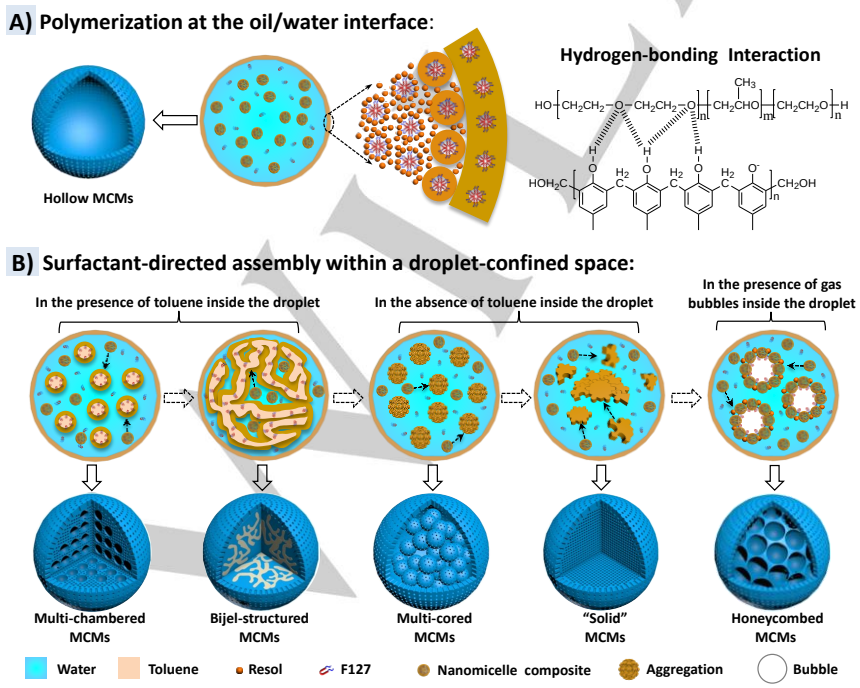

Figure 3. Schematic illustration of the formation mechanism of various interior-structured MCMs. A) Interfacial polymerization of phenolic resol in the presence of F127. B) Evolution of the interior structures.

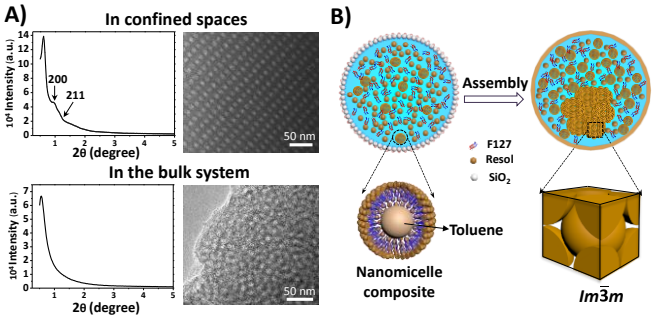

Figure 4. Comparisons of mesopore ordering of carbon materials synthesized in the confined system and in the bulk system, and mechanism for ordering enhancement. A) Small-angle XRD patterns and TEM images of carbon materials synthesized (0.4 mol L^{-1} NaOH, 100 °C, 30 wt% phenol) in droplet-confined spaces and in the bulk system. B) Formation of *Im*$\bar{3}$*m* mesostructure within the droplet-confined space.

restricted, the microphase change of the viscous liquids proceeds relatively slowly. This scenario benefits solidification and arresting of the structures of local metastable phases.[18a]

More impressively, the droplet-confined spaces also impact the mesopore ordering. As Figure 4A shows, even under exactly the same conditions, the small-angle XRD pattern of MCMs exhibits an apparent increase in the intensity of the (110) diffraction peak when compared to the material synthesized in the bulk system. Remarkably, the former clearly exhibits (200) and (211) diffraction peaks, while the latter does not. Such a periodicity enhancement is further confirmed by TEM observation (Figure 4A). Moreover, MCMs synthesized at other temperatures and base concentrations also exhibit significant enhancement in mesopore periodicity as compared to the materials synthesized in bulk (Figures S4E, S13 and S19). These findings point to the fact that a long-range mesopore ordering enhancement originates from the droplet-confined spaces. In the bulk system, the driving force for self-assembly is mainly dictated by weak interactions between nanomicelle composites, while in the droplet systems the confinement-induced entropy loss may help to improve the periodicity and promote the close packing of nanomicelle composites (Figure 4B), which was observed in silica–surfactant assemblies in the cylinder-confined system.[18c]

To verify the merits of these interior-structured MCMs, we examined their catalytic performance with the hydrogenation of levulinic acid to γ-valerolactone.[19] Ru nanoparticles (NPs, 2.0 nm; Figures S20A,B and S21A–C) were introduced into their mesopores through an impregnation method (Table S2), leading to catalysts for this reaction. It was found that the hydrogenation rate significantly depends on their interior structure although the selectivity was 100% in all cases (Figure S20C). After 80 min the conversion order is: Ru/MCMs (multi-cored, 99%) > Ru/MCMs (bijel-structured, 93%) > Ru/MCMs (multi-chambered, 85%) > Ru/MCMs ("solid", 78%). These differences should be attributed to the difference in diffusional transport within microspheres since both the experiment of varying stirring rate and the Weisz–Prater criterion (see notes in Figure S22) revealed that this reaction was limited by diffusion. To the best of our knowledge, this is the first attempt to improve the diffusivity of micron-sized carbon sphere-based catalysts through finely tuning their interior structures. Another attractive feature of these catalysts is easy separation from the reaction system through simple filtration, and does not require high-speed centrifugation. From the second to the sixth reaction cycle, the recovered Ru/MCMs (multi-cored) catalyst gave above 93% conversions. From the seventh to the tenth cycle, 87–96% conversions were still obtained through prolonging the reaction time (Figure S20D). The results of a hot filtration experiment show that the catalytic activity of the filtrate is very low and ca. 0.1 ppm Ru was detected in the filtrate (Figure S23). The recyclability of the Ru/MCMs was superior to that of a benchmarking catalyst Ru-supported commercial active carbon (Figures S24 and S25A). The Ru NPs size of the spent Ru/MCMs catalyst was determined to be ca. 2.2 nm (only slight increase in size, Figure S21D), which is much smaller than that of the benchmarking catalyst (5 nm, Figure S25B). This could be ascribed to the mesoporous structure that prevents the aggregation of Ru NPs.

Furthermore, MCMs can be incorporated with catalytically active sites even involving multi-components. After confirming that our protocol enables the synthesis of nitrogen (N)-functionalized MCMs (Figures S26–S28 and Table S6), we simultaneously introduced both N and Co elements into MCMs via a one-pot synthesis, expecting that Co nanoparticles (NPs) interact with N-rich carbon surfaces.[20a] The N, Co co-decorated catalyst was prepared via simple modification of the above synthesis protocol by adding $Co(OAc)_2{\cdot}4H_2O$ and melamine at the beginning (Figure S29). Nitroarene hydrogenation was used to evaluate these catalysts. Over the optimized catalyst Co/NMCMs-900 (900 means carbonization at 900 °C) with a 2.5 wt% Co loading, nitrobenzene was fully converted to aniline with > 99% selectivity within 3 h (Tables S3–S5). This catalyst worked well for other nitroarenes containing methyl, vinyl, methoxyl, amino, chloro- and bromo-substituents (Figure S30). 99% conversions and above 94% selectivity were obtained within 4–6 h. Its activity and selectivity are comparable to the reported catalysts prepared with expensive Co complex precursors or special supports such as carbon nanotubes.[20] The turn over number (TON) for ten reaction cycles reaches 982, which is even higher than most Co-based catalysts (Figures S31, S32 and Table S7).[20] The high activity and stability can be explained by the possibility that our synthesis protocol allows N and C precursors and Co salts to be mixed in water droplets at a molecular level, thus enhancing their strong interactions.

In summary, a method based on surfactant assembly within Pickering emulsion droplet has been successfully developed for the fabrication of uniform mesoporous carbon micrometer-sized spheres with complex interior structures. This approach allows the interior architecture to be easily tailored through adjustment of synthesis parameters, leading to a library of unprecedented interior-structured mesoporous carbon microspheres. Impressively, Pickering emulsion droplets were found to not only play an important role in the evolution of the complex interior structure but also significantly enhance the periodicity of mesoporous structures, suggesting a novel confinement effect. The interior-structured microspheres exhibited significantly enhanced diffusivity and ability to be separated, highlighting their superiority in technical applications. Moreover, this approach proves adaptable to fabrication of N-Co co-decorated MCMs catalysts via a one-pot synthesis, which exhibited excellent activity, selectivity and recyclability in the selective hydrogenation of nitroarenes. The results presented here open up new horizons in carbon materials as well as other inorganic materials research as they not only supply a novel avenue to fabrication of micron-sized spheres with complex interior

structures but also shed light on insights into the profound impact of the droplet-confined space on the evolution of the microstructure.

Acknowledgements

This work is supported by the Natural Science Foundation of China (21733009, 21573136 and U1510105), the Program for New Century Excellent Talents in University (NECT-12-1030), and the Program for Youth Sanjin Scholar.

Keywords: Pickering emulsions • surfactant assembly• carbon microspheres • mesoporous materials • confinement effects

[1] a) J. Liu, N. P. Wickramaratne, S. Z. Qiao, M. Jaroniec, *Nat. Mater.* **2015**, *14*, 763−774; b) D. S. Su, G. Wen, S. Wu, F. Peng, R. Schlogl, *Angew. Chem. Int. Ed.* **2017**, *56*, 936−964; c) A. D. Roberts, X. Li, H. F. Zhang, *Chem. Soc. Rev.* **2014**, *43*, 4341−4356; d) J. Schuster, G. He, B. Mandlmeier, T. Yim, K. T. Lee, T. Bein, L. F. Nazar, *Angew. Chem. Int. Ed.* **2012**, *51*, 3591−3595; e) S. Wang, W. C. Li, G. P. Hao, Y. Hao, Q. Sun, X. Q. Zhang, A. H. Lu, *J. Am. Chem. Soc.* **2011**, *133*, 15304−15307; f) B. Hu, K. Wang, L. Wu, S. H. Yu, M. Antonietti, M. M. Titirici, *Adv. Mater.* **2010**, *22*, 813−828; g) J. Liang, X. Zhang, L. Jing, H. Yang, *Chin. J. Catal.* **2017**, *38*, 1252−1260.

[2] a) Y. Han, Y. G. Wang, W. Chen, R. Xu, L. Zheng, J. Zhang, J. Luo, R. A. Shen, Y. Zhu, W. C. Cheong, C. Chen, Q. Peng, D. Wang, Y. Li, *J. Am. Chem. Soc.* **2017**, *139*, 17269−17272; b) F. Xu, Z. Tang, S. Huang, L. Chen, Y. Liang, W. Mai, H. Zhong, R. Fu, D. Wu, *Nat. Commun.* **2015**, *6*, 7221; c) G. Zheng, S. W. Lee, Z. Liang, H. W. Lee, K. Yan, H. Yao, H. Wang, W. Li, S. Chu, Y. Cui, *Nat. Nanotechnol.* **2014**, *9*, 618−623; d) H. Zhang, O. Noonan, X. Huang, Y. Yang, C. Xu, L. Zhou, C. Yu, *ACS nano* **2016**, *10*, 4579−4586; e) G. H. Wang, J. Hilgert, F. H. Richter, F. Wang, H. J. Bongard, B. Spliethoff, C. Weidenthaler, F. Schüth, *Nat. Mater.* **2014**, *13*, 293−300; f) C. J. Hofer, R. N. Grass, M. Zeltner, C. A. Mora, F. Krumeich, W. J. Stark, *Angew. Chem. Int. Ed.* **2016**, *55*, 8761−8765.

[3] R. Liu, S. M. Mahurin, C. Li, R. R. Unocic, J. C. Idrobo, H. Gao, S. J. Pennycook, S. Dai, *Angew. Chem. Int. Ed.* **2011**, *50*, 6799−6802.

[4] a) C. Zhang, H. B. Wu, C. Yuan, Z. Guo, X. W. Lou, *Angew. Chem. Int. Ed.* **2012**, *51*, 9592−9595; b) F. Böttger-Hiller, P. Kempe, G. Cox, A. Panchenko, N. Janssen, A. Petzold, T. Thurn-Albrecht, L. Borchardt, M. Rose, S. Kaskel, C. Georgi, H. Lang, S. Spange, *Angew. Chem. Int. Ed.* **2013**, *52*, 6088−6091; c) D. S. Bin, Z. X. Chi, Y. Li, K. Zhang, X. Yang, Y. G. Sun, J. Y. Piao, A. M. Cao, L. J. Wan, *J. Am. Chem. Soc.* **2017**, *139*, 13492−13498; d) X. Wang, J. Feng, Y. Bai, Q. Zhang, Y. Yin, *Chem. Rev.* **2016**, *116*, 10983−11060.

[5] a) Z. Wu, W. D. Wu, W. Liu, C. Selomulya, X. D. Chen, D. Zhao, *Angew. Chem. Int. Ed.* **2013**, *52*, 13764−13768; b) L. Guo, J. Zhang, Q. He, L. Zhang, J. Zhao, Z. Zhu, W. Wu, J. Zhang, J. Shi, *Chem. Commun.* **2010**, *46*, 7127−7129; c) B. Zhu, K. Li, J. Liu, H. Liu, C. Sun, C. E. Snape, Z. Guo, *J. Mater. Chem. A* **2014**, *2*, 5481−5489.

[6] a) K. W. Tan, B. Jung, J. G. Werner, E. R. Rhoades, M. O. Thompson, U. Wiesner, *Science* **2015**, *349*, 54−58; b) M. H. Sun, S. Z. Huang, L. H. Chen, Y. Li, X. Y. Yang, Z. Y. Yuan, B. L. Su, *Chem. Soc. Rev.* **2016**, *45*, 3479−3563; c) C. Yu, M. Chen, X. Li, C. Zhao, L. He, J. Qiu, *J. Mater. Chem. A* **2015**, *3*, 5054−5059; d) Y. Zhao, L. Jiang, *Adv. Mater.* **2009**, *21*, 3621−3638.

[7] B. C. Buddingh, J. C. M. van Hest, *Acc. Chem. Res.* **2017**, *50*, 769−777.

[8] a) S. E. Skrabalak, K. S. Suslick, *J. Am. Chem. Soc.* **2006**, *128*, 12642−12643; b) L. Zhang, X. Liu, Y. Dou, B. Zhang, H. Yang, S. Dou, H. Liu, Y. Huang, X. Hu, *Angew. Chem. Int. Ed.* **2017**, *56*, 13790−13794.

[9] a) J. Song, M. L. Gordin, T. Xu, S. Chen, Z. Yu, H. Sohn, J. Lu, Y. Ren, Y. Duan, D. Wang, *Angew. Chem. Int. Ed.* **2015**, *54*, 4325−4329; b) B. Wang, P. Prinsen, H. Wang, Z. Bai, H. Wang, R. Luque, J. Xuan, *Chem. Soc. Rev.* **2017**, *46*, 855−914; c) D. Zhang, J. Zhao, C. Feng, R. Zhao, Y. Sun, T. Guan, B. Han, N. Tang, J. Wang, K. Li, J. Qiao, J. Zhang, *J. Power Sources* **2017**, *342*, 363−370; d) M. Li, Y. Zhang, X. Wang, W. Ahn, G. Jiang, K. Feng, G. Lui, Z. Chen, *Adv. Funct. Mater.* **2016**, *26*, 8408−8417.

[10] J. Zhou, Z. Sun, M. Chen, J. Wang, W. Qiao, D. Long, L. Ling, *Adv. Funct. Mater.* **2016**, *26*, 5368−5375.

[11] M. Zhang, L. Wei, H. Chen, Z. Du, B. P. Binks, H. Yang, *J. Am. Chem. Soc.* **2016**, *138*, 10173−10183.

[12] a) Y. Yang, Z. Wei, C. Wang, Z. Tong, *ACS Appl. Mater. Interfaces* **2013**, *5*, 2495-2502; b) M. Li, R. L. Harbron, J. V. Weaver, B. P. Binks, S. Mann, *Nat. Chem.* **2013**, *5*, 529-536.

[13] T. Y. Ma, L. Liu, Z. Y. Yuan, *Chem. Soc. Rev.* **2013**, *42*, 3977−4003.

[14] Y. Meng, D. Gu, F. Zhang, Y. Shi, H. Yang, Z. Li, C. Yu, B. Tu, D. Zhao, *Angew. Chem. Int. Ed.* **2005**, *44*, 7053−7059.

[15] C. Huang, J. Forth, W. Wang, K. Hong, G. S. Smith, B. A. Helms, T. P. Russell, *Nat. Nanotechnol.* **2017**, *12*, 1060−1063.

[16] M. Zhang, R. Ettelaie, T. Yan, S. Zhang, F. Cheng, B. P. Binks, H. Yang, *J. Am. Chem. Soc.* **2017**, *139*, 17387−17396.

[17] a) R. Ameloot, F. Vermoortele, W. Vanhove, M. B. Roeffaers, B. F. Sels, D. E. De Vos, *Nat. Chem.* **2011**, *3*, 382−387; b) B. P. Binks, J. H. Clint, P. D. I. Fletcher, S. Rippon, S. D. Lubetkin, P. J. Mulqueen, *Langmuir* **1999**, *15*, 4495−4501.

[18] a) M. F. Haase, J. Brujic, *Angew. Chem. Int. Ed.* **2014**, *53*, 11793−11797; b) G. Astarloa-Aierbe, J. M. Echeverría, A. Vázquez, I. Mondragon, *Polymer* **2000**, *41*, 3311−3315; c) Y. Wu, G. Cheng, K. Katsov, S. W. Sides, J. Wang, J. Tang, G. H. Fredrickson, M. Moskovits, G. D. Stucky, *Nat. Mater.* **2004**, *3*, 816−822.

[19] F. Liguori, C. Moreno-Marrodan, P. Barbaro, *ACS Catal.* **2015**, *5*, 1882−1894.

[20] a) F. A. Westerhaus, R. V. Jagadeesh, G. Wienhofer, M. M. Pohl, J. Radnik, A. E. Surkus, J. Rabeah, K. Junge, H. Junge, M. Nielsen, A. Bruckner, M. Beller, *Nat. Chem.* **2013**, *5*, 537−543; b) T. Schwob, R. Kempe, *Angew. Chem. Int. Ed.* **2016**, *55*, 15175−15179; c) P. Zhou, L. Jiang, F. Wang, K. Deng, K. Lv, Z. Zhang, *Sci. Adv.* **2017**, *3*, e1601945; d) Z. Wei, J. Wang, S. Mao, D. Su, H. Jin, Y. Wang, F. Xu, H. Li, Y. Wang, *ACS Catal.* **2015**, *5*, 4783−4789.

COMMUNICATION

*Dawei Liu, Nan Xue, Lijuan Wei, Ye Zhang, Mingxing Tang, Zhangfeng Qin, Xuekuan Li, Bernard P. Binks and Hengquan Yang**

Surfactant Assembly within Pickering Emulsion Droplets for Fabrication of Interior-Structured Mesoporous Carbon Microspheres

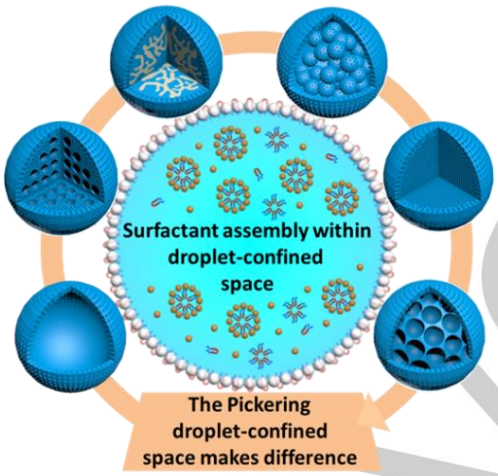

Confinement is powerful: Surfactant assembly within Pickering droplet-confined spaces makes a difference in the fabrication of inorganic microspheres. It is demonstrated that a library of mesoporous carbon microspheres (MCMs) including hollow MCMs, multi-cored MCMs, multi-chambered MCMs, bijel-structured MCMs, honeycombed MCMs and "solid" MCMs come into the world.

This is the peer reviewed version of the following article: B. Jiao, A. Shi, Q. Wang, B. P. Binks, Angew. Chem. Int. Ed. 2018, 57, 9274, which has been published in final form at https://doi.org/10.1002/anie.201801350. This article may be used for non-commercial purposes in accordance with Wiley Terms and Conditions for Use of Self-Archived Versions.